Flight-Test Maneuver Modeling and Control

P. K. A. Menon*
Georgia Institute of Technology, Atlanta, Georgia
R. A. Walker†
FMC Central Engineering Laboratory, Santa Clara, California
and
E. L. Duke‡
NASA Ames-Dryden Flight Research Facility/OFDC, Edwards, California

The use of automated flight-test schemes decreases the aircraft flight testing time and pilot work load while enhancing the data quality. Two major elements involved in developing such an automated technique are maneuver modeling to generate command histories from maneuver specifications, and the synthesis of control systems to track these command histories. This paper describes these two aspects of the automated flight-test scheme for a high-peformance fighter aircraft. A suboptimal minimum error excitation linear-quadratic-regulator approach is used for maneuver autopilot synthesis. Closed-loop simulation results are given.

Introduction

THE interest in automated flight-test trajectory control arises from its demonstrated potential for decreasing the flight test in time and pilot work load while enhancing the quality of collected data. In Ref. 1, for instance, through manned simulations it was shown that a trajectory guidance scheme is particularly beneficial for those tasks that require the pilot to integrate information from multiple sensors. In that work an open-loop system with the pilot closing the control loop was used in the evaluations. An alternate strategy is to synthesize a completely automatic closed-loop system with the pilot in a supervisory role. Such an approach was adopted in Ref. 2, wherein a closed-loop flight-test trajectory controller was synthesized using full-state feedback linear-quadratic-regulator theory.

In order to circumvent the difficulties in implementing a full-state feedback regulator, an output feedback design with constrained eigenstructure assignment technique was discussed in Ref. 3. The work reported in Refs. 2 and 3 has included detailed modeling of all the aircraft subsystems for control-law development. These investigations have identified maneuver modeling as a significant aspect of the flight-test trajectory control problem needing further clarification and development. The maneuver modeling aspect of the trajectory guidance problem will be emphasized in this paper. The maneuvers described here are designed to generate aircraft performance, and the engine data for subsequent analysis to aid in refining the prediction methods. Some of these maneuvers have never been discussed before in the literature.

There are at least two approaches for maneuver modeling. First, one could iteratively simulate the nonlinear aircraft model until the open-loop controls generate the desired output histories. Or, second, one can trim the aircraft model at a number of flight conditions close to the desired trajectory and approximately compute the commanded trajectory using these trim values. The second approach is followed in this paper mainly because of the number of trajectories that had to be flown. The former approach is practical only if a very limited number of trajectories are to be executed. In order to characterize the aircraft nonlinearities, a table of straight and level trim conditions and level turn trim conditions spanning the aircraft flight envelope is first constructed. In the present case, 64 straight and level trims, 51 level turn trims at a load factor of 2, and 30 level turn trims at a load factor of 4 were employed. The independent variables in this trim table are Mach number, altitude, and the load factor. Using a three-dimensional interpolation scheme, the lift, drag, engine thrust, angle of attack, body attitudes and corresponding rates, and the control surface settings at an intermediate flight condition can be calculated. The maneuver commands are then generated using this data in conjunction with simplified aircraft modeling. Some maneuver modeling details will be discussed in the next section.

In this paper, a closed-loop mechanization of the flight-test trajectory controller will be considered, with the pilot in a supervisory role. Using a numerical linearization program such as the one described in Ref. 4, the aircraft model at a given Mach altitude load-factor point can be generated. This linear model can then be used to synthesize a controller to maintain the aircraft close to the desired trajectory. Because of the large parameter changes in the aircraft model as it traverses throught the various trim points, a gain schedule scheme is essential for satisfactory operation. In the present case, the gains were scheduled as a function of Mach number, altitude, and load factor. The details of the controller synthesis will be given in one of the following sections. We note here than an alternate control system design technique based on nonlinear inverses[5] is feasible for the flight-test trajectory control problem. A brief discussion on the advantages and disadvantages of the present work when compared to that in Ref. 5 will be given in the section on maneuver autopilot design.

Maneuver Modeling

The objective of maneuver modeling is to generate a consistent set of state and control histories to serve as commands and open-loop control settings for the maneuver autopilot, using a data base consisting of trim conditions. Two sets of trim conditions have been found adequate for all the maneuers considered in this paper: straight and level trims and level turn trims. To the extent feasible, kinematic relationships are employed to generate the commanded state histories. Whenever this is not feasible, linearized aerodynamics and engine models are employed. Note that the following development is not restricted to any particular aircraft. In the present

Presented as Paper 86-0426 at the AIAA 24th Aerospace Science Meeting, Reno, NV, Jan. 6-9, 1986; received Jan. 20, 1986; revision received Oct. 5, 1987.

*Associate Professor. Member AIAA.
†Manager, High Speed Processing. Member AIAA.
‡Aerospace Engineer. Member AIAA.

work, the commands and the open-loop controls consists of 1) Commands: altitude, Mach number, angle of attack, flight-path angle, roll altitude, roll-pitch-yaw body rates, and 2) Open-loop controls: throttle, elevator, rudder, and differential tail.

In the following, the maneuver modeling for three flight-test trajectories will be discussed in detail. A few more maneuver models are given in Ref. 6. Note that the open-loop controls generated by the present maneuver modeling approach are approximate. The chief motivation in employing these approximations is to minimize the amount of on-line computer storage.

Zoom and Pushover Maneuver

The zoom and pushover trajectory is a wings-level thrust-stabilized less than 1-g maneuver. The flight-test trajectory is a parabolic path with the target Mach-altitude angle-of-attack point at the apex. The primary objective in this maneuver is to generate aircraft performance data at angles of attack less than the level flight trim values for validating wind-tunnel and computational fluid dynamics predictions.

This is one of the more complex symmetric flight maneuvers. The flight-test trajectory consists of three phases. In the first phase, the aircraft is transferred from its straight and level initial condition to the beginning of the parabolic flight path. At this point, the throttle is fixed and the aircraft executes the zoom and pushover maneuver. This is the second phase. In the third phase, the aircraft is brought back to its initial conditions using a transient trajectory. A schematic of this flight-test maneuver is given in Fig. 1. The first and third phases are essentially transient trajectories mechanized using a cubic polynomial history for altitude, i.e.,

$$h = h_o + a_1 t + a_2 t^2 + a_3 t^3, \qquad t_o \le t \le t_f \tag{1}$$

In this expression, h is the altitude at any time t, h_o the initial altitude, and t_f the final time. The requirement for a cubic polynomial is clear, since one may attempt to meet four boundary conditions on altitude, viz., the initial and final altitudes and their rates may all be specified. To simplify the development, constant acceleration, or deceleration along the flight path is assumed next. However, if one desires to meet additional boundary conditions on the airspeed rates, the use of a higher-order polynomial in time may be considered. With the assumption of constant acceleration, one has the following expression for airspeed:

$$V = V_o + \dot{V}t, \qquad \dot{V} = \frac{V_f - V_o}{V_f} \tag{2}$$

Here, V_f is the specified final airspeed, V_o the initial airspeed, and t_f the final time. The flight-path angle γ along this maneuver is readily computed from

$$\gamma = \sin^{-1}\left[\frac{a_1 + 2a_2 t + 3a_3 t^2}{V_o + \dot{V}t}\right] \tag{3}$$

Next, assuming that the lift is close to weight throughout this maneuver, the angle-of-attack history can be generated by interpolating between stored straight and level trim data at the Mach-altitude pairs given by Eqs. (1) and (2). Approximate open-loop control surface settings may similarly be obtained. The open-loop throttle setting required to generate the desired acceleration/deceleration, however, will have to be computed using force balance, as follows. Assuming that the aerodynamic drag along this maneuver is close to the straight and level trim values, the thrust required can be calculated as

$$T = \frac{(\dot{V} + g\sin\gamma)m + D}{\cos\alpha} \tag{4}$$

In Eq. (4), T is the thrust required to generate the desired acceleration $\dot{V}$, α the angle of attack, m the aircraft mass, and g the acceleration due to gravity. The open-loop throttle setting may be computed from the thrust T by assuming that the thrust-throttle characteristic is linear. It is important to stress here that this assumption is found to result in less than 3% error for the aircraft under consideration. First, the maximum thrust at the current Mach-altitude condition is computed as

$$T_{\max} = \frac{T_{\text{trim}}}{\eta_{\text{trim}}} \tag{5}$$

In Eq. (5), the subscript max denotes the maximum value of thrust, the subscript trim denotes the values at the straight and level trim conditions, and the variable η is the throttle setting. The open-loop throttle settings may be computed from

$$\eta_{\text{actual}} = \frac{T}{T_{\max}} \tag{6}$$

The roll-pitch-yaw body rates are expected to be small during this maneuver and, consequently, the corresponding commands are zero. If the throttle setting emerging from this analysis is greater than the maximum or less than the minimum, it indicates that the assumed time of flight for the maneuver is unrealistic. In that case, this quantity has to be changed appropriately to make the maneuver feasible.

The zoom and pushover phase of this flight-test trajectory will use the three well-known properties of a parabolic flight path: 1) horizontal acceleration is zero, 2) vertical acceleration is constant, and 3) total energy is constant.

Since the apex speed is specified, say V_T, one has

$$\dot{x} = V\cos\gamma = V_T = \text{const}$$

Here, x is the downrange. From this,

$$\gamma = \pm\cos^{-1}\left(\frac{V_T}{V}\right) \tag{7}$$

The sign in Eq. (7) can be chosen based on whether the aircraft is flying toward the apex or away from it.

From the given apex speed, the angle of attack, and altitude, the lift and drag can be computed using the linearized aerodynamic coefficients from the straight and level trim data table. From the constant energy property, at the apex of the parabola, one has

$$T\cos\alpha = D \tag{8}$$

The thrust required at the apex can be calculated since the angle of attack and drag are known. Using this value of thrust, the throttle setting is calculated by invoking the linear thrust-throttle relationship and using Eqs. (5) and (6). This throttle setting will be maintained constant throughout the second phase. With known values of lift and thrust, the vertical acceleration at the apex can be computed as

$$\frac{T\sin\alpha + L}{m} - g = g_a \tag{9}$$

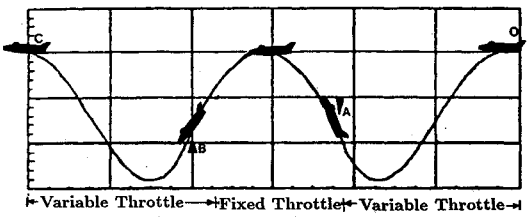

Fig. 1 Zoom and pushover flight-test trajectory.

The quantity g_a is negative, numerically less than the acceleration due to gravity g. The vertical acceleration g_a has to remain constant throughout the parabolic path. The total energy of the aircraft along the trajectory is given by

$$E = h + \frac{V^2}{-2g_a} = \text{const} \tag{10}$$

As the total energy is to remain constant during the zoom and pushover maneuver, Eq. (10) may be used to compute the speed along the parabolic path, given the altitude.

Next, given the altitude at which the parabolic trajectory is to begin, and perhaps end, one can write

$$h = h_o + \dot{h}_o t + \frac{g_a}{2} t^2 \tag{11}$$

The initial altitude rate $\dot{h}_o$ can be computed from

$$\dot{h}_o = \sqrt{-2g_a(E-h_o)}\,\sin[\pm\cos^{-1}(V_T/V_o)] \tag{12}$$

The time of flight on the parabola is next calculated as

$$t_f = \frac{2}{-g_a}\sqrt{V_o^2 - V_T^2} \tag{13}$$

The angle-of-attack command along the parabolic path can then be calculated using

$$\alpha = [m(g_a + g\cos\gamma) - L_o]/(T + L_\alpha) \tag{14}$$

Equation (14) used small-angle approximation for α to simplify the computations. Along the zoom and pushover maneuver, the open-loop control surface settings used are the interpolated values from the straight and level trim data table.

Constant Dynamic Pressure, Constant Load Factor Trajectory

This maneuver is initiated at a predetermined load factor, Mach number, and dynamic pressure. It can either be an ascending or descending maneuver at a specified Mach rate. The dynamic pressure and load factor are held constant throughout this maneuver. Altitude is gained or lost to maintain the dynamic pressure with changing Mach number. The primary motivation in flying this maneuver is to generate data for validating wind-tunnel predictions.

This trajectory is executed in three phases. Beginning at a straight and level flight condition at the desired dynamic pressure, the aircraft is first placed in a steady level turn at the required load factor. During the second phase, the desired Mach rate is achieved along with an altitude rate to maintain the dynamic pressure-load factor conditions. In the third phase, the aircraft is returned to straight and level conditions. A typical negative Mach-rate trajectory is illustrated in Fig. 2. In the following, the constant dynamic pressure-constatnt load factor maneuver will be discussed, since the first and the third phases can be constructed by mere interpolation of the level turn trim data table.

Differentiating the expression for dynamic pressure Q with respect to time, and using the altitude rate equation, with $\dot{Q}=0$, one has

$$\dot{V} = -\frac{1}{2\rho}\frac{\partial\rho}{\partial h} V^2 \sin\gamma \tag{15}$$

Next, differentiating the expression for Mach number $M = V/C$ with respect to time, and substituting for altitude rate,

$$\dot{V} = \dot{M}C + \frac{V^2}{C}\frac{\partial C}{\partial h}\sin\gamma \tag{16}$$

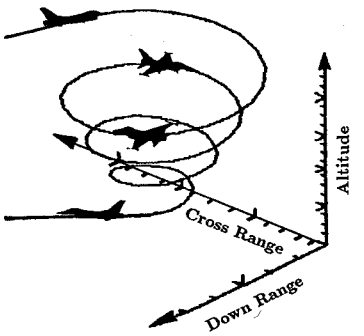

Fig. 2 Negative Mach rate, constant dynamic pressure: constant load factor flight-test trajectory.

Equating Eqs. (15) and (16), the flight-path angle required to maintain the dynamic pressure constant while generating a desired Mach rate turns out to be

$$\gamma = \sin^{-1}\left[-\dot{M}C/V^2\left(\frac{1}{2\rho}\frac{\partial\rho}{\partial h} + \frac{1}{C}\frac{\partial C}{\partial h}\right)\right] \tag{17}$$

There are two conclusions that can be drawn from Eq. (17):

1) Because $\partial\rho/\rho h$ and $\partial C/\partial h$ are negative, a positive $\dot{M}$ will result in a climbing trajectory, while a negative $\dot{M}$ will yield a descending path.

2) This maneuver cannot be flown at atitudes where $\partial\rho/\partial h$ and $\partial C/\partial h$ are nearly zero unless the desired Mach rate is also zero.

The flight-path angle given by Eq. (17) may be substituted in the altitude rate equation and numerically integrated to obtain the commanded state variable histories. The open-loop throttle setting is computed from the level turn trim thrust and throttle setting at the current Mach-altitude load factor as follows:

$$T = \left[g - \frac{1}{2\rho}\frac{\partial\rho}{\partial h}V^2\right]\frac{m\sin\gamma}{\cos\alpha} + \frac{D}{\cos\alpha} \tag{18}$$

The throttle setting corresponding to this thrust at the current flight conditions can be computed using Eqs. (5) and (6). The angle of attack and drag in Eq. (18) are the interpolated values from the trim data table at the current Mach-altitude load factor condition. The Mach number as a function of time is obtained from

$$M = M_o + \dot{M}t \tag{19}$$

In Eq. (19), M_o is the initial Mach number, $\dot{M}$ the desired Mach rate, and t the time. The commanded values of body rates and open-loop control surface deflections are again the interpolated values from the level turn trim data table.

Constant Reynolds Number, Constant Load Factor Trajectory

The objective in this maneuver is to maintain the load factor and Reynolds number constant while maintaining a desired Mach rate. The data collected in this flight-test trajectory are used for validating wind-tunnel predictions. This maneuver model is different from the constant dynamic pressure-constant load factor trajectory only in the way that one computes the flight-path angle and the required thrust. Hence, only these two aspects will be discussed in the following. The Reynolds number R_e is given by

$$R_e = \frac{Vd\rho}{\mu} \tag{20}$$

Here, d is the characteristic length and μ the absolute viscosity of air specified as a function of altitude. Differentiating Eq.

(20) with respect to time and using the altitude rate equation, with $\dot{R}_e = 0$, one has

$$\dot{V} = \left[\frac{1}{\mu}\frac{\partial \mu}{\partial h} - \frac{1}{\rho}\frac{\partial \rho}{\partial h}\right] V^2 \sin\gamma \tag{21}$$

Equating Eq. (21) to Eq. (16)

$$\gamma = \sin^{-1}\left[\dot{M}C/V^2\left(\frac{1}{\mu}\frac{\partial \mu}{\partial h} - \frac{1}{\rho}\frac{\partial \rho}{\partial h} - \frac{1}{C}\frac{\partial C}{\partial h}\right)\right] \tag{22}$$

As in the constant dynamic presure-constant load factor flight-test trajectory, this maneuver cannot be flown at the altitude where $\partial u/\partial h$, $\partial \rho/\partial h$, and $\partial C/\partial h$ are close to zero unless the desired Mach rate is also zero.

The open-loop throttle setting can be computed from the level turn trim thrust drag and throttle setting at the current Mach-altitude load factor, using the thrust required, calculated using the expression

$$T = \left[\left(\frac{1}{\mu}\frac{\partial \mu}{\partial h} - \frac{1}{\rho}\frac{\partial \rho}{\partial h}\right) V^2 + g\right]\frac{m \sin\gamma}{\cos\alpha} + \frac{D}{\cos\alpha} \tag{23}$$

in conjunction with Eqs. (5) and (6).

Maneuver Autopilot Design

The previous section described maneuver modeling that generates the commands to be tracked by the maneuver autopilot. This section will deal with the synthesis of the maneuver autopilot for maintaining the aircraft close to the commanded trajectories. A popular approach for designing closed-loop controllers for flight vehicles consists of linearizing the vehicle model about the desired operating point and applying one of the several linear synthesis techniques. In the case where the flight vehicle is to follow a desired trajectory, the linearization is carried out at several points on the desired trajectory and controllers designed. The controllers are then scheduled so that the overall closed-loop system response meets the time response and accuracy specifications. Note that this is a multivariable control problem and has to be treated as such.

A nonlinear controller synthesis approach for the flight-test trajectory control problem was discussed in Ref. 5. In the present paper, the controller synthesis will be based on a more traditional approach via the linear system theory. Before proceeding further, a brief comparison between the two will be presented. The chief advantage of linear perturbation controllers is that their implementation requires relatively minor on-line calculations. The disadvantages are that they require gain scheduling and storage of nominal control setting along the desired trajectory. Additionally, they may demand mode switching for handling various flight maneuvers. The nonlinear controllers, on the other hand, demand complex on-line calculations and a significant amount of data storage, but do not required gain scheduling. Moreover, in this case, the controller synthesis can be carried out using the single-input single-output linear system theory. Note that both approaches require the maneuver modeling to generate commanded trajectories.

From an implementation point of view, the synthesis techniques that produce output feedback controllers are preferable over full state-feedback techniques. An earlier attempt in this direction using the eigenstructure assignment,[3,7] though successful, was found too cumbersome for repeated use. The difficulty in using eigenstructure assignment in the present situation is primarily one of selecting a set of eigenvectors and eigenvalues that would produce a stable output feedback system. Although this approach is quite attractive for unaugmented aircraft wherein the system modes are easily recognizable, it is difficult to apply in the present case due to the presence of an extremely complex 31-state command augmentation system. The approach employed in this paper is originally due to Kosut,[8] and permits one to obtain an output feedback controller from a full-state feedback controller generated via the linear-quadratic regulator theory.[9] Two distinct approximation techniques have been outlined in Ref. 8: the minimum norm approximation and the minimum error excitation approach. The latter was selected for the present application due to the larger degree of freedom it offers. In the following, an outline of this approach will be given.

Following Kosut's[8] notation for the minimum error excitation approach, for the linear system

$$\dot{x} = Ax + Bu \tag{24}$$

$$y = Hx \tag{25}$$

with $x \epsilon R^n$, $u \epsilon R^m$, and A, B, H being real constant matrices of compatible dimensions, one first designs a full-state regulator minimizing the performance index

$$J = \frac{1}{2}\int_0^\infty (x^T Q x + u^T R u)\,dt \tag{26}$$

This process yields an optimal feedback control law of the form

$$u^* = F^* x \tag{27}$$

Next, a Lyapunov equation of the form

$$(A + BF^*)P + P(A + BF^*)^T + I = 0 \tag{28}$$

is solved to obtain the constrained feedback gain as

$$C = F^* P H^T (HPH^T)^{-1} \tag{29}$$

The output feedback controller is then of the form

$$u = Cy \tag{30}$$

In the foregoing and in all that follows, the superscript T denotes the transpose operation.

Because this output feedback synthesis method does not guarantee stability, and because of the presence of either neutrally stable unobservable modes or other sluggish phugoid-like or integral error modes, it is desirable to carry out this design with a guaranteed eigenvalue margin.[9] Specifying an eigenvalue margin of κ ensures that the real parts of all the closed-loop poles are less than κ. This is equivalent to synthesizing a full-state regulator with the modified performance index

$$J = \frac{1}{2}\int_0^\infty e^{-2\kappa t}(x^T Q x + u^T R u)\,dt \tag{31}$$

This can be accomplished by destabilizing the open-loop plant by $A = A + \kappa I$ and solving for the optimal gains in the standard linear-quadratic-regulator problem. It is interesting to note that in Ref. 10 such an approach was used for the design of an implicit model following control system for the X-22A V/STOL aircraft. In the present problem, the matrices Q and R in the performance index (31) were selected according to Bryson's rule,[11] i.e., the inverse of the squared deviation desired on the controls and outputs with a scalar factor between Q and R to regulate the extent of high-gain solution achieved. Since we are interested in the trajectory tracking problem, the variables x and u in Eqs. (24–31) should be interpreted as the perturbations in the nominal state and control variables, i.e.,

$$x = x - x_a, \qquad u = u - u_a \tag{32}$$

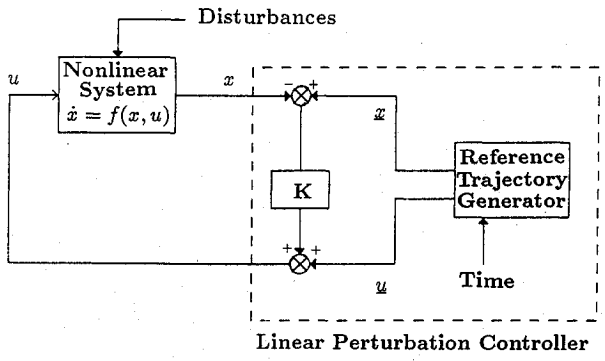

Fig. 3 Implementation of the linear perturbation controller.

where x and u are the state and control variables along the nominal trajecotry, and x_a and u_a are the actual aircraft state and control variables.

With the above methodology, maneuver autopilot design could be accomplished in two or three iterations at any particular flight condition. The design specifications used in the present case were that the real part of all the eigenvalues should be less than or equal to -0.2, and that the damping ratio of the slowest complex conjugate root should be about 0.7. To realize adequate command tracking, integral error feedback was introduced in the angle of attack, airspeed, and roll attitude channels. About 20 controllers were synthesized at various flight conditions within the aircraft flight envelope. These controllers are then scheduled as a function of Mach number, altitude, and load factor. A schematic of the controller implementation is shown in Fig. 3. In the next section, the performance of these controllers along one of the flight-test trajectories will be presented.

Simulation Results

For the purposes of illustration, the controller performance along a descending constant Reynold's number-constant load factor trajectory will be given here. The aircraft, starting from 35,000 ft and Mach 1.2 straight and level flight conditions, is first placed in a tightening level turn to achieve the desired load factor. At this point the desired Mach rate is commanded along with the altitude rate to maintain constant Reynolds number. In the present case, the commanded Mach rate was -0.0067/s and required the aircraft to descend to about 30,000 ft in 30 s. At the end of the constant Reynolds number-constant load factor maneuver, the aircraft is returned to the straight and level condition at the new Mach number-altitude condition. Note that this is a relatively severe maneuver requiring the aircraft to lose speed while descending in a 4-g turn with about -10 deg flight-path angle.

A linear time varying simulation of the aircraft and the flight-test trajectory controller was set up to generate the results given in this section. Figure 4 gives the commanded and actual altitude and Mach number histories along the constant Reynolds number-constant load factor maneuver. The Reynolds number evolution along this trajectory is given in Fig. 5. Throughout the trajectory, the Reynolds number is maintained within 1.5% of the required value. Note that the Reynolds number given in Fig. 5 has to be multiplied by the characteristic length d to obtain the actual Reynolds number. The throttle setting and the elevator deflection along this maneuver are given in Fig. 6. The elevator deflection approaches saturation at the point where the Mach rate command is initiated, at about 30 s in Fig. 6. Though the controller performance has been evaluated along several other flight-test trajectories, they could not all be presented here. However, these simulations revealed that the maneuver autopilot synthesized in this work meets all the required maneuver accuracy specifications.

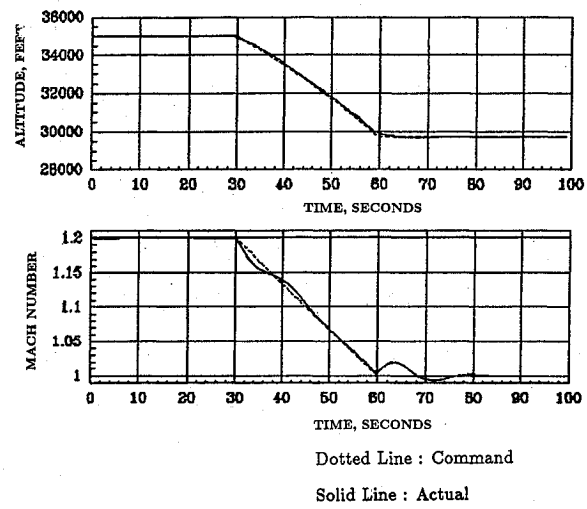

Fig. 4 Altitude and Mach number evolution along the constant Reynolds number, constant load factor flight-test trajectory (dotted line: command; solid line: actual).

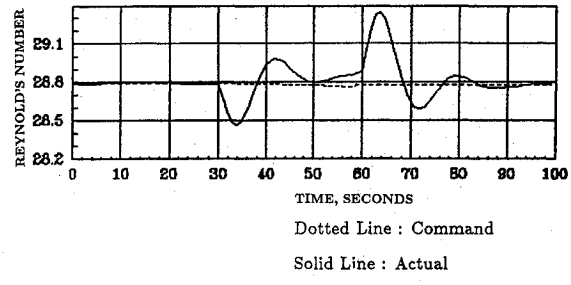

Fig. 5 Reynolds number evolution along the constant Reynolds number: constant load factor flight-test trajectory (dotted line: command; solid line: actual).

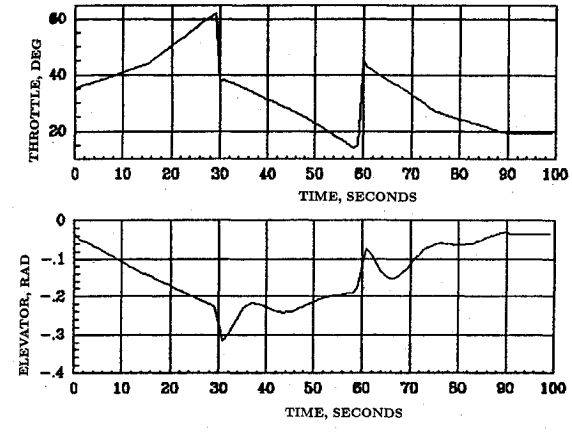

Fig. 6 Throttle and elevator deflection along the constant Reynolds number: constant load factor flight-test trajectory.

Conclusions

This paper described the development of an automated flight-test scheme for aircraft that decreases the flight testing time and pilot work load while enhancing the data quality. Two major elements involved in developing such an automated technique, the maneuver modeling to generate command histories from the maneuver specifications and the synthesis of control systems to track these command histories were discussed in detail. Specifically, the maneuver modeling for three flight-test trajectories using a table of straight and level trim data and level turn trim data in conjunction with

simplified aircraft models was outlined. This modeling generates the commands and open-loop controls for the maneuver autopilot. The maneuver autopilot synthesis with Kosut's[8] suboptimal minimum error excitation linear-quadratic-regulator approach was given. Finally, the performance of the controller along the constant Reynolds number-constant load factor flight-test trajectory was evaluated in a closed-loop simulation. The controller implementation in a manned aircraft simulation and flight test is currently underway.

Acknowledgments

This research was supported by NASA Ames-Dryden Flight Research Facility under Contract NAS2-11877. Thanks are due to Mr. Robert F. Antoniewicz of NASA Dryden for help in using the computer program given in Ref. 4. The authors thank the referees for their constructive criticism of this paper. This work was completed when the first two authors were with Integrated Systems, Santa Clara, California.

References

[1]Duke, E. L., Swann, M. R., Enevoldson, E. K., and Wolf, T. D., "Experience with Flight Test Trajectory Guidance," *Journal of Guidance, Control, and Dynamics,* Vol. 6, Sept.-Oct. 1983, pp. 393-398.

[2]Walker, R. A. and Gupta, N. K., "Flight Test Trajectory Control Analysis," NASA CR-170395, Feb. 1983.

[3]Menon, P. K. A., Saberi, H. A., Walker, R. A., and Duke, E. L., "Flight Test Trajectory Controller Synthesis with Eigenstructure Assignment," American Control Conference, Boston, MA, June 1985.

[4]Duke, E. L. and Antoniewicz, R. F., "Development and Validation of a General Purpose Linearization Program for Rigid Aircraft Needs, "AIAA Paper 85-1891-CP., Aug. 1985.

[5]Menon, P. K. A., Badgett, M. E., Walker, R. A., and Duke, E. L., "Nonlinear Flight Test Trajectory Controllers for Aircraft," *Journal of Guidance, Control, and Dynamics,* Vol. 10, Jan.-Feb. 1987, pp. 67-72.

[6]Menon, P. K. A. and Walker, R. A., "Aircraft Flight Test Trajectory Control, " ISI Rept. N. 56, prepared for NASA Ames-Dryden Flight Research Center under Contract NAS2-11877, Oct. 1985.

[7]Shapiro, E. Y. and Chung, J. C., "Constrained Eigenvalue/Eigenvector Assignment-Application to Flight Control Systems," 24th Israel Annual Conf. on Aviation and Astronautics, Tel-Aviv, Israel, Feb. 1984.

[8]Kosut, R. L., "Suboptimal Control of Linear Time-Invariant Systems Subject to Control Structure Constraints," *IEEE Transactions on Automatic Control,* Vol. AC-15, Oct. 1970, pp. 557-563.

[9]Anderson, B. D. O. and Moore, J. B., *Linear Optimal Control,* Prentice-Hall, Englewood Cliffs, NJ, 1971.

[10]Lebacqz, J. V. and Govindaraj, K. S., "Implicit Model Following and Parameter Identification of Unstable Aircraft," *Journal of Guidance, Control, and Dynamics,* Vol. 3, March-April 1980, pp. 119-123.

[11]Bryson, A. E., "Kalman Filter Divergence and Aircraft Motion Estimators," Dept. of Aeronautics and Astronautics, Stanford Univ., Stanford, CA, SUDDAR-505, July 1977.